Chapter 5

FIRST-ORDER CHANNEL STATISTICS

The received power in fading wireless channels fluctuates between maxima and minima as a function of space, time, and frequency. A wireless engineer must accept the fact that for certain regions in space, time, or frequency, the receiver may have to operate with received signal strength below an acceptable *signal-to-noise* or *signal-to-interference* ratio. To quantify the effects of a fading channel on receiver performance, we must first quantify the distribution of received power or voltage envelope that a receiver experiences in a randomly selective channel.

This chapter develops the principles of first-order analysis for stochastic frequency-selective and spatially selective radio channels. The most important tool in a first-order analysis is the probability density function (PDF). In developing the use of a PDF for modeling random channels, the chapter discusses the following key points:

- Section 5.1: Discussion of mean received power.

- Section 5.2: Construction of envelope PDFs for I-SLAC models.

- Section 5.3: Analytical solutions to I-SLAC envelope PDFs.

- Section 5.4: Analysis of the two-wave with diffuse power (TWDP) PDF.

- Section 5.5: Summary of important concepts.

This chapter uses the definitions and concepts from the preceding chapters to develop many of the classical distributions used in wireless engineering to describe small-scale fading. Furthermore, new fading distributions that augment the classical understanding are developed and discussed. Indeed, the SLAC model defined in Chapter 4 is shown to produce an incredible variety of first-order channel behavior.

5.1   Mean Received Power

Of all first-order statistics to calculate for stochastic channel model, mean received power is perhaps the most common. Regardless of other statistical fading properties, mean received power is an intuitive measure of receiver performance, since, according to information theory, received power is related to the fundamental limitations on the amount of information that can be sent through a noisy channel [Cov91].

5.1.1   Average Versus Received Power

Consider a SLAC model with three constant-amplitude waves. Movement in frequency or space causes a steady phase rotation of each, as illustrated in Figure 5.1. Different components rotate at different speeds and directions (clockwise or counterclockwise in Figure 5.1). When the three waves are summed from one moment to the next, the composite signal undergoes constructive-destructive interference. In this way, the total envelope of a received radio signal is rarely near its average value. The distribution of a random envelope process about its average level has a dramatic effect on radio link performance. Thus, this chapter presents a thorough discussion of the moments and the PDFs of envelope processes.

5.1.2   Stationarity

Stationarity is one of the most important and powerful attributes to determine in a stochastic model. There are many different types of stationarity (we have already discussed *wide-sense stationarity* in previous chapters). In fact, the term *stationary* may be used to describe any type of statistic that is invariant of channel dependencies. For example, a time-varying process is *mean stationary* if its mean value does not change as a function of time.

Often, statistics of an entire *order* are said to be stationary. The *order* of a statistic refers to the number of stochastic process samples used in its calculation. For example, the autocorrelation function is a *second-order* statistic because it is calculated from two samples of the stochastic process, as shown in Equation (3.1.2). One sample is taken at t_1 and the other sample is taken at t_2.

In this chapter, it is useful to establish *first-order stationarity* in the stochastic channel models. A process is first-order stationary if all of its first-order statistics - mean, variance, PDF, and so on - are invariant of the dependencies space and frequency. The U-SLAC model is a first-order stationary channel model, which makes it a convenient tool for analytical channel description. This trait of the U-SLAC model is proven in Theorem 5.1.

Theorem 5.1: First-Order Stationarity

Statement: The U-SLAC model is first-order stationary.
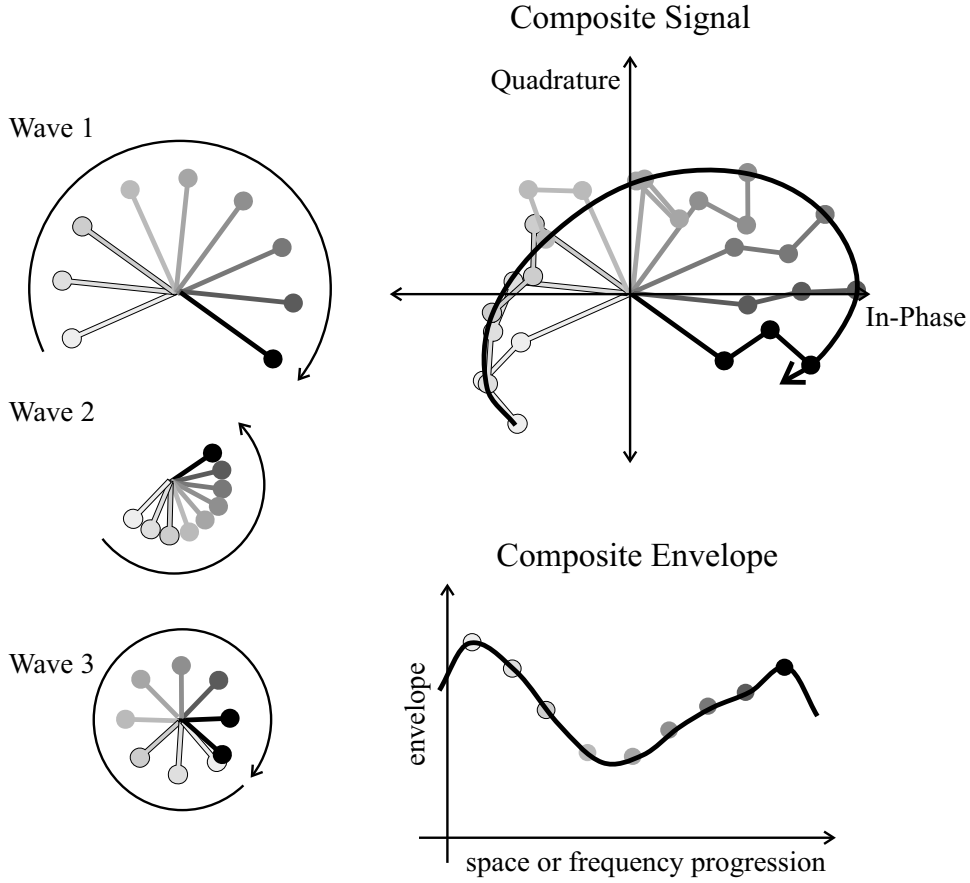
Composite Signal

Figure 5.1 Example of three specular waves that add to form a small-scale fading channel.

Proof: Consider the U-SLAC model of Equation (4.4.1) evaluated at frequency $f = 0$ and position $\vec{r} = \vec{0}$. The resulting channel expression is shown below

$$\tilde{h}(0,\vec{0}) = \sum_{i=1}^{N} V_i \exp\left(j\left[\Phi_i - \vec{k}_i \cdot \vec{r} - 2\pi f \tau_i\right]\right)\Bigg|_{\substack{f = 0 \\ \vec{r} = \vec{0}}} = \sum_{i=1}^{N} V_i \exp(j\Phi_i)$$

$$(5.1.1)$$

Now consider the case of the channel evaluated at any arbitrary point in frequency, f, and space, $\vec{r}$. By making the following substitution,

$$\Phi_i' = \left(\Phi_i - \vec{k}_i \cdot \vec{r} - 2\pi f \tau_i\right) \bmod 2\pi$$

we could express the U-SLAC model in the following form:

$$\tilde{h}(f, \vec{r}) = \sum_{i=1}^{N} V_i \exp(j\Phi_i') \qquad (5.1.2)$$

The random phases, $\{\Phi_i'\}$, in Equation (5.1.2) are the same set of random phases, $\{\Phi_i\}$, in Equation (5.1.1) with arbitrary constants added. Otherwise, the two equations look identical. Since a uniform phase random variable remains uniformly distributed if any arbitrary constant is added to it, the expressions in Equation (5.1.1) and Equation (5.1.2) are identically distributed random variables. Adding the constant does not change the cyclical correlation properties, either. Thus, the distribution of values for $\tilde{h}(f, \vec{r})$ is identical and independent of frequency, f, and position, $\vec{r}$ - the definition of first-order stationary.

Note: Confusion of Order and Moments

The difference between the *orders* and the *moments* of a stochastic process causes endless confusion. The term *moment* refers to a family of first order statistics. For example, $\mathrm{E}\{R(f,\vec{r})\}$, $\mathrm{E}\{R(f,\vec{r})^2\}$, and $\mathrm{E}\{R(f,\vec{r})^3\}$ are the first, second, and third moments of the envelope process $R(f,\vec{r})$ - but all three are first-*order* statistics.

The most sweeping type of stationarity is *strict-sense stationary* (SSS) behavior. A stochastic process is SSS if it is stationary with respect to every order. While establishing SSS behavior in a process is highly desirable, it is extremely difficult to prove in most types of stochastic processes. The I-SLAC model is an exception, as Theorem 5.2 demonstrates.

Theorem 5.2: Strict-Sense Stationarity

Statement: The I-SLAC model is strict-sense stationary.

Proof: Consider a simple stochastic channel consisting of a single wave term:

$$\tilde{h}_1(f, \vec{r}) = V_1 \exp\left(j\left[\Phi_1 - \vec{k}_1 \cdot \vec{r} - 2\pi f \tau_1\right]\right)$$

where V_1 is a constant amplitude and Φ_1 is a random phase variable, uniformly distributed over the interval $[0, 2\pi)$. This process is SSS [Pap91, p. 301]. Since the sum of two independent SSS processes will produce an SSS process, the following process

$$\tilde{h}_2(f, \vec{r}) = \tilde{h}_1(f, \vec{r}) + V_2 \exp\left(j\left[\Phi_2 - \vec{k}_2 \cdot \vec{r} - 2\pi f \tau_2\right]\right)$$

is SSS provided the random phase variable, Φ_2, is independent of Φ_1 (as it is in an I-SLAC model). An arbitrary number of independent wave components may be added in this manner and, by induction, any I-SLAC model may be constructed and shown to be an SSS process.

It is probably evident now why we draw a distinction between SLAC, U-SLAC, and I-SLAC models: The nature of the phase distributions in the model of Equation (4.4.1) (arbitrary, uncorrelated, or independent) determines the level of stationarity. A SLAC model may be nonstationary with respect to every statistic. A U-SLAC model, however, is guaranteed to be at least WSS (Theorem 4.2 and Theorem 5.1). An I-SLAC model is guaranteed to be stationary with respect to *every* order and statistic (Theorem 5.2).

5.1.3 Mean U-SLAC Power

For a WSS U-SLAC model, it is possible to calculate a closed-form expression for the mean received power, $P(f, \vec{r})$. Inserting the SLAC model expression into the definition of mean received power produces

$$\mathrm{E}\left\{P(f,\vec{r})\right\} = \mathrm{E}\left\{|\tilde{h}(f,\vec{r})|^2\right\}$$

$$= \sum_{l=1}^{N}\sum_{m=1}^{N} V_l V_m \underbrace{\mathrm{E}\left\{\exp\left(j\left[\Phi_l - \Phi_m\right]\right)\right\}}_{=\,0\ \text{for}\ l\neq m} \exp\left(j\left[(\vec{k}_m - \vec{k}_l)\cdot\vec{r} + 2\pi(\tau_m - \tau_l)f\right]\right)$$

$$= \sum_{m=1}^{N} V_m^2 \tag{5.1.3}$$

The expectation in the second line of Equation (5.1.3) is zero for $m \neq l$ by definition of a U-SLAC process. The end result of Equation (5.1.3) may be stated in words as follows: The mean power in a U-SLAC model is equal to the sum of the powers carried by the individual multipath waves [Rap02a]. Stated this way, Equation (5.1.3) can be considered a type of conservation-of-power law.

5.1.4 Frequency and Spatial Averaging

In the application of first-order statistics to real-life problems, it is important to speak of *averaging*. This is particularly true when attempting to measure the local area channel. In practice, it is not possible to generate an infinitum of realizations and calculate an ensemble. Rather, it is most feasible to average a measured statistic over a single realization.

This averaging may occur over each dependency of the measured channel. For example, sweeping a narrowband transmitted carrier over a range of frequencies and measuring the received voltage is a form of *frequency averaging*. Mathematically, we will define the operation of frequency averaging as

$$\left\langle\ \cdot\ \right\rangle_f = \lim_{B\to\infty}\frac{1}{B}\int_{-B/2}^{B/2}(\ \cdot\ )\,df \tag{5.1.4}$$

In this definition, a statistic is calculated by averaging the value over the range of all allowable frequencies. In practice, the integration of Equation (5.1.4) cannot be taken over an infinite range.

A similar definition exists for spatial averaging. Mathematically, we will define the operation of spatial averaging as

$$\Big\langle \; \cdot \; \Big\rangle_{\vec{r}} = \lim_{L \to \infty} \frac{1}{L^3} \int\limits_{-L/2}^{L/2} (\; \cdot \;) \; d\vec{r} \tag{5.1.5}$$

where the integration in Equation (5.1.5) is a threefold integration over the x, y, and z coordinates.

5.1.5   Ergodicity

Stochastic processes with statistics that exhibit *ergodicity* are particularly useful for measurements and analysis of real-world processes. A statistic is said to be ergodic if, when measured by averaging a single realization of a stochastic ensemble, it is equal to the ensemble average. For example, a process is *mean-ergodic* if the frequency- and spatially-averaged mean of a single realization equals the ensemble-averaged mean. We express mean ergodicity for a stochastic channel as

$$\text{Condition for Mean Ergodicity: } \left\langle \left\langle \tilde{h}(f, \vec{r}) \right\rangle_{\vec{r}} \right\rangle_f = \text{E} \left\{ \tilde{h}(f, \vec{r}) \right\}$$

Of course, this property must hold for *all* realizations of $\tilde{h}(f, \vec{r})$ in the stochastic ensemble.

Since there are two dependencies in the SLAC model - frequency and space - it is convenient to describe ergodicity with respect to each individual dependency. For example, it is possible that a statistic is ergodic with respect to frequency but not space. The converse is also possible. The basic principles governing the frequency and spatial ergodicity of mean received power are summarized in Theorem 5.3.

Theorem 5.3: Power Ergodicity

Statement:

1. A U-SLAC model is power-ergodic with respect to frequency if its scattering is heterogeneous with respect to frequency.

2. A U-SLAC model is power-ergodic with respect to space if its scattering is heterogeneous with respect to space.

3. All U-SLAC models with heterogeneous scattering are power-ergodic with respect to both space and frequency.

Proof:

1. The frequency averaged power of any SLAC model is given by inserting Equation (4.4.1) into the frequency-averaging operation defined in Equation (5.1.4):

$$
\begin{aligned}
\langle P(f,\vec{r})\rangle_f &= \left\langle |\tilde{h}(f,\vec{r})|^2 \right\rangle_f \\
&= \sum_{l=1}^{N}\sum_{m=1}^{N} V_l V_m \exp\left(j\left[\Phi_l - \Phi_m + (\vec{\mathrm{k}}_m - \vec{\mathrm{k}}_l)\cdot\vec{r}\right]\right) \\
&\quad \times \underbrace{\left\langle \exp\left(j2\pi[\tau_m - \tau_l]f\right)\right\rangle_f}_{=\,0 \text{ for } \tau_m \neq \tau_l}
\end{aligned}
\tag{5.1.6}
$$

If all delays, $\{\tau_i\}$, in the SLAC model are heterogeneous (dissimilar), then the result in Equation (5.1.6) reduces to

$$
\langle P(f,\vec{r})\rangle_f = \sum_{m=1}^{N} V_m^2
\tag{5.1.7}
$$

which is the ensemble average for power in a U-SLAC model.

2. The spatially averaged power of any SLAC model is given by inserting Equation (4.4.1) into the space-averaging operation defined in Equation (5.1.5):

$$
\begin{aligned}
\langle P(f,\vec{r})\rangle_{\vec{r}} &= \left\langle |\tilde{h}(f,\vec{r})|^2 \right\rangle_{\vec{r}} \\
&= \sum_{l=1}^{N}\sum_{m=1}^{N} V_l V_m \exp\left(j\left[\Phi_l - \Phi_m + 2\pi(\tau_m - \tau_l)f\right]\right) \\
&\quad \times \underbrace{\left\langle \exp\left(j[\vec{\mathrm{k}}_m - \vec{\mathrm{k}}_l]\cdot\vec{r}\right)\right\rangle_{\vec{r}}}_{=\,0 \text{ for } \vec{\mathrm{k}}_m \neq \vec{\mathrm{k}}_l}
\end{aligned}
\tag{5.1.8}
$$

If all wavevectors, $\{\vec{\mathrm{k}}_i\}$, in the SLAC model are heterogeneous (dissimilar), then the result in Equation (5.1.8) reduces to

$$
\langle P(f,\vec{r})\rangle_{\vec{r}} = \sum_{m=1}^{N} V_m^2
\tag{5.1.9}
$$

which is also the ensemble average for power in a U-SLAC model.

3. This result follows logically from 1 and 2.

An immediate consequence of Theorem 5.3 is the equivalence of averaging received power with respect to frequency or space. If a SLAC model has heterogeneous scattering, then the following result holds:

$$
\langle P(f,\vec{r})\rangle_f = \langle P(f,\vec{r})\rangle_{\vec{r}}
\tag{5.1.10}
$$

In other words, received power averaged as a function of frequency produces the same result as received power averaged as a function of space. Both are equal to the ensemble-averaged power of the U-SLAC model that describes the location.

This equivalence is particularly powerful when *measuring* local area power in a real-life radio channel. The experimentalist has the freedom to calculate mean power in a channel measurement by using

(a) a wideband transmitted signal and a fixed-antenna receiver [Rap02a].

(b) a narrowband transmitted signal and a receiver antenna moving in space [Dur98b].

For case (a), the mean power is calculated from the received power averaged over the frequencies in the wideband signal. For case (b), the mean power is calculated from the received power averaged at the different receiver positions in space. The two techniques are equivalent.

Note: Importance of Heterogeneous Scattering

By now it is clear why Chapter 4 introduced the concept of *heterogeneous scattering*. Heterogeneous scattering is a crucial property for determining ergodicity. Ergodicity is a crucial property for determining the "measurability" of a real channel. Hence, the property of heterogeneous scattering determines how statistics may be calculated from a real-world channel measurement.

5.2   Envelope Probability Density Functions

Mean received power is just one aspect of first-order stochastic channel behavior. To understand the complete first-order behavior, it is necessary to calculate the power or envelope PDF. This section describes the generation of PDFs for a variety of I-SLAC models.

5.2.1   Notes and Concepts

The PDFs developed in this section are strictly for I-SLAC models. In order to derive a deterministic expression for the distribution of received power or voltage envelope, it is necessary to have a uniquely defined joint PDF on the phases of a SLAC model. A U-SLAC model, which only asserts uncorrelated phases, is not restrictive enough for this criterion. The I-SLAC model, with its independent, uniformly distributed phases, does have a specific joint PDF describing phases.

Furthermore, the envelope PDFs of this section are based on the *reduced wave grouping* (see Section 4.3.4). As will become apparent later, envelope PDFs involving a diffuse, nonspecular component depends only on the mean-squared power of that component - not the fine multipath wave structure within the component. Thus, when constructing a PDF from an arbitrarily complicated I-SLAC model, the reduced wave grouping may be used without loss of generality.

Finally, all of the PDFs presented in this chapter are with respect to received voltage envelope. If a distribution with respect to received power is desired, the envelope PDF may be converted to a power PDF. Since envelope, R, is simply equal to the square root of power, P, the following relationships hold:

Converting envelope PDF to power PDF: $\quad f_P(\mathrm{p}) = \dfrac{1}{2\sqrt{\mathrm{p}}} f_R(\sqrt{\mathrm{p}}) \quad$ (5.2.1)

Converting power PDF to envelope PDF: $\quad f_R(\rho) = 2\rho f_P(\rho^2) \qquad$ (5.2.2)

Most wireless journal papers, as a convention, report envelope PDFs.

5.2.2 Characteristic Functions

Since the reduced wave grouping of Equation (4.3.4) is a sum of independent random variables, the envelope PDF may be found by using a characteristic function approach. Recall from probability theory that if a real-valued random variable, Z, is the sum of a set of independent random variables, $\{W_i\}$:

$$Z = \sum_i W_i$$

then the characteristic function of Z - the Fourier transform of the PDF - is equal to the product of the characteristic functions of each individual W_i random variable [Pap91].

The same characteristic function technique may be used for the independent, *complex* random variable terms that constitute an I-SLAC model. The diffuse, nonspecular term and the N specular terms of Equation (4.3.4) are independent complex variables, each having a characteristic function, $\Phi_{XY}(v)$. The product of these individual characteristic functions may then be transformed into a PDF describing the envelope of Equation (4.3.4).

The PDF of a scalar random variable and its characteristic function are Fourier transform pairs. Since fading PDFs are functions of *envelope*, and since complex *voltages* must be summed as phasors, the transforms for an envelope PDF, $f_R(\rho)$, and its characteristic function, $\Phi_{XY}(v)$, are modified to the following expressions, as shown in Appendix 5.A:

$$\Phi_{XY}(v) = \int\limits_0^\infty f_R(\rho) \mathrm{J}_0(v\rho)\, d\rho \qquad (5.2.3)$$

$$f_R(\rho) = \rho \int\limits_0^\infty \Phi_{XY}(v) \mathrm{J}_0(v\rho)\, v\, dv \qquad (5.2.4)$$

To solve the problem of constructing envelope PDFs for a reduced wave grouping, we must only find the characteristic functions of specular components and diffuse components.

> *Note: The Fourier-Bessel Transform*
>
> Equation (5.2.3) and Equation (5.2.4) define a transform pair in the form of a *Fourier-Bessel* transform. Also called the *Hankel* transform, the formal relationship is defined for the following pair:
>
> $$\frac{f_R(\rho)}{\rho} \longleftrightarrow \Phi_{XY}(\upsilon)$$

5.2.3   Specular Characteristic Function

A specular voltage term of the form $V_0 \exp(j\Phi_0)$ has constant amplitude, V_0, and uniformly random phase, Φ_0. The envelope of this term is always V_0, regardless of the phase. Therefore, the envelope PDF of a specular component is best described by a delta function:

$$f_R(\rho) = \delta(\rho - V_0) \tag{5.2.5}$$

Plugging this function into the transform in Equation (5.2.3) produces the specular characteristic function:

$$\Phi_{XY}(\upsilon) = \mathrm{J}_0(V_0 \upsilon) \tag{5.2.6}$$

Thus, the characteristic function of a specular wave component is a zero-order Bessel function that depends only on the amplitude of the specular component [Ben48].

5.2.4   Diffuse, Nonspecular Characteristic Function

Diffuse, nonspecular received voltage may be written as the sum of numerous small-valued wave components.

$$
\begin{aligned}
\tilde{V}_{\mathrm{dif}} &= \sum_{i=1}^{N} V_i \exp(j\Phi_i) \\
&= \sum_{i=1}^{N} V_i \cos \Phi_i \quad + \quad j\sum_{i=1}^{N} V_i \sin \Phi_i \\
&= X + jY
\end{aligned}
\tag{5.2.7}
$$

which may be grouped into in-phase, X, and quadrature, Y, random variables. In the limit of large N, the real and imaginary components of $\tilde{V}_{\mathrm{dif}}$ follow the central limit theorem, each tending to zero-mean, identically distributed Gaussian distributions. Provided all the individual amplitudes, $\{V_i\}$, remain small relative to the total power, the distributions of X and Y will be uncorrelated. Thus, the joint distribution may be written as

$$f_{XY}(x, y) = \frac{1}{2\pi\sigma^2} \exp\left(-\frac{x^2 + y^2}{2\sigma^2}\right) \tag{5.2.8}$$

where σ^2 is the variance of X and Y.

The probability that the random envelope, R, of the diffuse, nonspecular voltage is below a level ρ is defined as the *cumulative density function* (CDF). The envelope CDF, $F_R(\rho)$, may be calculated from the joint distribution, $f_{XY}(x, y)$, by performing the following integration:

$$F_R(\rho) = \Pr\left[R < \rho\right] = \int\limits_0^{2\pi} \int\limits_0^{\rho} f_{XY}(\rho'\cos\phi, \rho'\sin\phi)\rho' d\rho' d\phi \qquad (5.2.9)$$

Equation (5.2.9) has a simple geometrical interpretation. If we view the in-phase component, X, and quadrature component, Y, as coordinates on a Cartesian plane, then the envelope, R, is simply the Pythagorian distance to the origin, $R = \sqrt{X^2 + Y^2}$. Thus, the probability that the envelope will be less than a threshold value ρ is equal to the integration of the joint PDF over a circular region centered at the origin with radius ρ. Equation (5.2.9) performs this integration.

The PDF is simply the derivative of the CDF. Differentiation of Equation (5.2.9) produces

$$f_R(\rho) = \frac{dF_R(\rho)}{d\rho} = \rho \int\limits_0^{2\pi} f_{XY}(\rho\cos\phi, \rho\sin\phi)d\phi \qquad (5.2.10)$$

To obtain the PDF of the diffuse, nonspecular voltage component, we insert the joint Gaussian PDF of Equation (5.2.8) into Equation (5.2.10). This produces the following PDF:

$$
\begin{aligned}
f_R(\rho) &= \frac{\rho}{2\pi\sigma^2} \int\limits_0^{2\pi} \exp\left(-\frac{(\rho\cos\phi)^2 + (\rho\sin\phi)^2}{2\sigma^2}\right) d\phi \\
&= \frac{\rho}{\sigma^2} \exp\left(-\frac{\rho^2}{2\sigma^2}\right) \\
&= \frac{2\rho}{P_{\text{dif}}} \exp\left(-\frac{\rho^2}{P_{\text{dif}}}\right) \qquad (5.2.11)
\end{aligned}
$$

The substitution $P_{\text{dif}} = 2\sigma^2$ is made to give the PDF more physical meaning. The value P_{dif} is the mean power of the nonspecular voltage component,

$$P_{\text{dif}} = \text{E}\left\{\left|\tilde{V}_{\text{dif}}\right|^2\right\}$$

where $\tilde{V}_{\text{dif}}$ is the diffuse component. The power, P_{dif}, is less nebulous than the value σ.

The final step simply involves plugging the diffuse, nonspecular envelope PDF into Equation (5.2.3) to produce the characteristic function

$$\Phi_{XY}(\upsilon) = \exp\left(-\frac{\upsilon^2 P_{\text{dif}}}{4}\right) \qquad (5.2.12)$$

Thus, the characteristic function of a diffuse, nonspecular voltage component is a Gaussian-shaped function that depends only on the average power of the voltage component, P_{dif} [Ric44], [Ric45]. The distribution of amplitudes, $\{V_i\}$, is not important - only the mean-squared power affects the shape of this characteristic function.

5.2.5   The I-SLAC PDF Generator

Now that the characteristic functions for specular components and diffuse, nonspecular components have been determined, it is possible to construct an envelope PDF for the reduced wave grouping by chaining the characteristic functions together and inverting the product using Equation (5.2.4). The general form for the I-SLAC envelope PDF of the reduced wave grouping, Equation (4.3.4), is given by

$$f_R(\rho) = \rho \int\limits_{0}^{\infty} \mathrm{J}_0(\upsilon\rho) \exp\left(\frac{-\upsilon^2 P_{\text{dif}}}{4}\right) \left[\prod_{i=1}^{N} \mathrm{J}_0(V_i \upsilon)\right] \upsilon \, d\upsilon \qquad (5.2.13)$$

$$\text{for} \quad R = \left|\tilde{V}_{\text{dif}} + \sum_{i=1}^{N} V_i \exp(j\Phi_i)\right| \quad \text{and} \quad \mathrm{E}\left\{|\tilde{V}_{\text{dif}}|^2\right\} = P_{\text{dif}}$$

which is valid for $\rho \geq 0$. Equation (5.2.13) allows for *any* combination of single, constant-amplitude voltage waves and a diffuse group of voltage waves. As the next section demonstrates, Equation (5.2.13) has a number of closed-form solutions that result from standard definite integrals [Abr70], [Gra94].

5.3   Closed-Form PDF Solutions

There are five different types of reduced wave groupings that produce closed-form solutions for the envelope PDF generator in Equation (5.2.13). This section describes the five PDFs and discusses their use in wireless communications. Table 5.1 summarizes these cases.

5.3.1   The One-Wave PDF

A trivial case of fading is the *one-wave PDF*, in which only one constant-amplitude wave is present in a local area. Its characteristic function, however, is a building block for other canonical fading PDFs. Integrating Equation (5.2.13) for $N = 1$ and $P_{\text{dif}} = 0$ produces a result of 0 for all values of r except $r = V_1$, which is infinite [Abr70, p. 485]. Thus, the PDF is represented by

$$f_R(\rho) = \delta(\rho - V_1) \qquad (5.3.1)$$

The one-wave PDF, as illustrated in the IQ plot of Figure 5.2, results in no envelope fading.

Table 5.1 Summary of Envelope PDFs in Different Fading Environments

PDF	Expression for Envelope PDF $f_R(\rho)$	Characteristic Function $\Phi_{XY}(v)$	$\mathrm{E}\{R\}$ (volts)	$\mathrm{E}\{R^2\}$ (volts^2)
One-Wave No Fading	$\delta(\rho - V_1)$	$\mathrm{J}_0(V_1 v)$	V_1	V_1^2
Two-Wave Simple Fading	$\dfrac{2\rho}{\pi\sqrt{4V_1^2 V_2^2 - (V_1^2 + V_2^2 - \rho^2)^2}}$ $\|V_1 - V_2\| \leq \rho \leq V_1 + V_2$	$\mathrm{J}_0(V_1 v)\mathrm{J}_0(V_2 v)$	$\dfrac{2(V_1+V_2)}{\pi}\mathrm{E}\!\left[\dfrac{4V_1 V_2}{(V_1+V_2)^2}\right]$	$V_1^2 + V_2^2$
Three-Wave† Max. Discrete Fading	$\dfrac{\rho^{\frac{1}{2}}}{\pi^2\sqrt{V_1 V_2 V_3}}K\!\left(\dfrac{\Delta_\rho^2}{V_1 V_2 V_3 \rho}\right),\ \Delta_\rho^2 < V_1 V_2 V_3 \rho^*$ $\dfrac{\rho}{\pi^2 \Delta_\rho}K\!\left(\dfrac{V_1 V_2 V_3 \rho}{\Delta_\rho^2}\right),\ \Delta_\rho^2 < V_1 V_2 V_3 \rho^*$	$\mathrm{J}_0(V_1 v)\mathrm{J}_0(V_2 v)\mathrm{J}_0(V_3 v)$	no closed-form solution	$V_1^2 + V_2^2 + V_3^2$
Rayleigh Numerous Multipath	$\dfrac{2\rho}{P_{\mathrm{dif}}}\exp\!\left(\dfrac{-\rho^2}{P_{\mathrm{dif}}}\right)\mathrm{u}(\rho)$	$\exp\!\left(\dfrac{-v^2 P_{\mathrm{dif}}}{4}\right)$	$\sqrt{\dfrac{\pi P_{\mathrm{dif}}}{4}}$	P_{dif}
Rician Dominant Component	$\dfrac{2\rho}{P_{\mathrm{dif}}}\exp\!\left(\dfrac{-\rho^2 - V_1^2}{P_{\mathrm{dif}}}\right)\mathrm{I}_0\!\left(\dfrac{2V_1\rho}{P_{\mathrm{dif}}}\right)\mathrm{u}(\rho)$	$\mathrm{J}_0(V_1 v)\exp\!\left(\dfrac{-v^2 P_{\mathrm{dif}}}{4}\right)$	no closed-form solution	$P_{\mathrm{dif}} + V_1^2$

* also provided that $2\max(V_1, V_2, V_3) - V_1 - V_2 - V_3 \leq \rho \leq V_1 + V_2 + V_3$; otherwise $f_R(\rho) = 0$.

† $16\Delta_\rho^2 = \left[(\rho + V_1)^2 - (V_2 - V_3)^2\right]\left[(V_2 + V_3)^2 - (\rho - V_1)^2\right]$

$K(x)$ – Complete First Kind Elliptical Integral $E(x)$ – Complete Second Kind Elliptical Integral

$\mathrm{J}_n(x)$ – Bessel Function $\mathrm{I}_n(x)$ – Modified Bessel Function
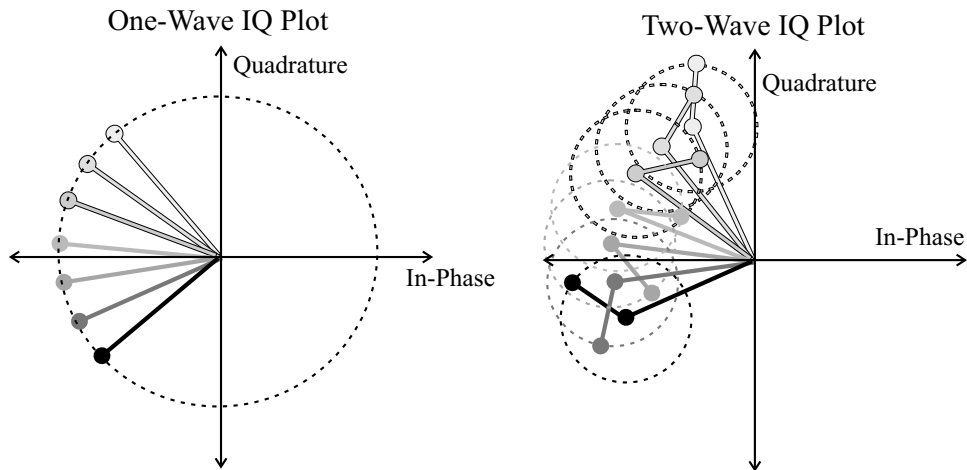
One-Wave IQ Plot

Two-Wave IQ Plot

Figure 5.2 IQ plots of a single specular wave with no envelope fading (left) and two specular waves with constructive-destructive interference (right).

5.3.2   The Two-Wave PDF

The *two-wave PDF* represents the envelope fading caused by the interference of only two constant-amplitude waves in a local area, corresponding to $N = 2$ and $P_{\mathrm{dif}} = 0$ in Equation (5.2.13). Integration of Equation (5.2.13) under these conditions is a well-understood result that produces the following PDF [Gra94, p. 718]:

$$f_R(\rho) = \frac{2\rho}{\pi\sqrt{4V_1^2 V_2^2 - (V_1^2 + V_2^2 - \rho^2)^2}}, \quad |V_1 - V_2| \le \rho \le V_1 + V_2 \qquad (5.3.2)$$

Equation (5.2.13) evaluates to zero for $\rho < |V_1 - V_2|$ and $\rho > V_1 + V_2$, leading to the limits placed on ρ in Equation (5.3.2). Figure 5.2 shows an IQ sketch of two-wave envelope fading.

Figure 5.3 plots several examples of the two-wave PDF and CDF using a convenient parameter, Δ, which we have defined to relate the amplitudes of V_1 and V_2 to one another [Dur99c]. The Δ-parameter ranges between 0 and 1 and is defined by

$$\Delta = \frac{\text{Peak Specular Power}}{\text{Average Specular Power}} - 1 = \frac{2V_1 V_2}{V_1^2 + V_2^2} \qquad (5.3.3)$$

As shown in Figure 5.3, when the magnitudes of two multipath waves are equal, $\Delta = 1$. In the absence of a second component (V_1 or $V_2 = 0$), $\Delta = 0$. For dissimilar voltage values, the two-wave PDF exhibits two prominent spikes, which mark the interval over which the PDF is nonzero. For the limiting case of $\Delta = 1$ ($V_1 = V_2$), the lower spike disappears and the PDF permits envelope values of zero, which correspond to complete destructive cancellation.

Example 5.1: Mean of a Two-Wave PDF

Problem: Calculate the mean of a fading envelope that follows a two-wave distribution with voltages V_1 and V_2.

Solution: The mean of the two-wave distribution follows from the basic integral:

$$\mathrm{E}\left\{R\right\} = \int\limits_{0}^{\infty} \rho f_R(\rho)\, d\rho$$

After inserting Equation (5.3.2) for $f_R(\rho)$, we write

$$\mathrm{E}\left\{R\right\} = \int\limits_{|V_1 - V_2|}^{V_1 + V_2} \frac{2\rho^2\, d\rho}{\pi\sqrt{4V_1^2 V_2^2 - (V_1^2 + V_2^2 - \rho^2)^2}}$$

This problem becomes much easier after a clever change of integration variables, $\rho = \sqrt{V_1^2 + V_2^2 + 2V_1 V_2 \sin(2\theta)}$. This substitution produces the following simplification:

$$\begin{aligned}
\mathrm{E}\left\{R\right\} &= \frac{2}{\pi} \int\limits_{-\frac{\pi}{4}}^{\frac{\pi}{4}} \sqrt{V_1^2 + V_2^2 + 2V_1 V_2 \sin(2\theta)}\, d\theta \\[2mm]
&= \frac{2(V_1 + V_2)}{\pi} \underbrace{\int\limits_{0}^{\frac{\pi}{2}} \sqrt{1 + \frac{4V_1 V_2}{(V_1 + V_2)^2} \sin^2(\theta)}\, d\theta}_{\mathrm{E}\left(\frac{4V_1 V_2}{(V_1 + V_2)^2}\right)}
\end{aligned}$$

Thus, the final answer may be expressed in terms of a complete elliptic integral of the second kind (see Appendix A.5). Note that, as in all other cases, it is much easier to calculate the power mean from the two-wave distribution than the envelope mean. Following Equation (5.1.3), the average two-wave power is simply $V_1^2 + V_2^2$.

5.3.3   The Three-Wave PDF

Two- and three-wave models often are used to describe fading in microwave digital radio communications [Rum86]. The *three-wave PDF* in Table 5.1 is the solution of Equation (5.2.13) for $N = 3$ and $P_{\mathrm{dif}} = 0$, a result formulated by Nicholson in 1920
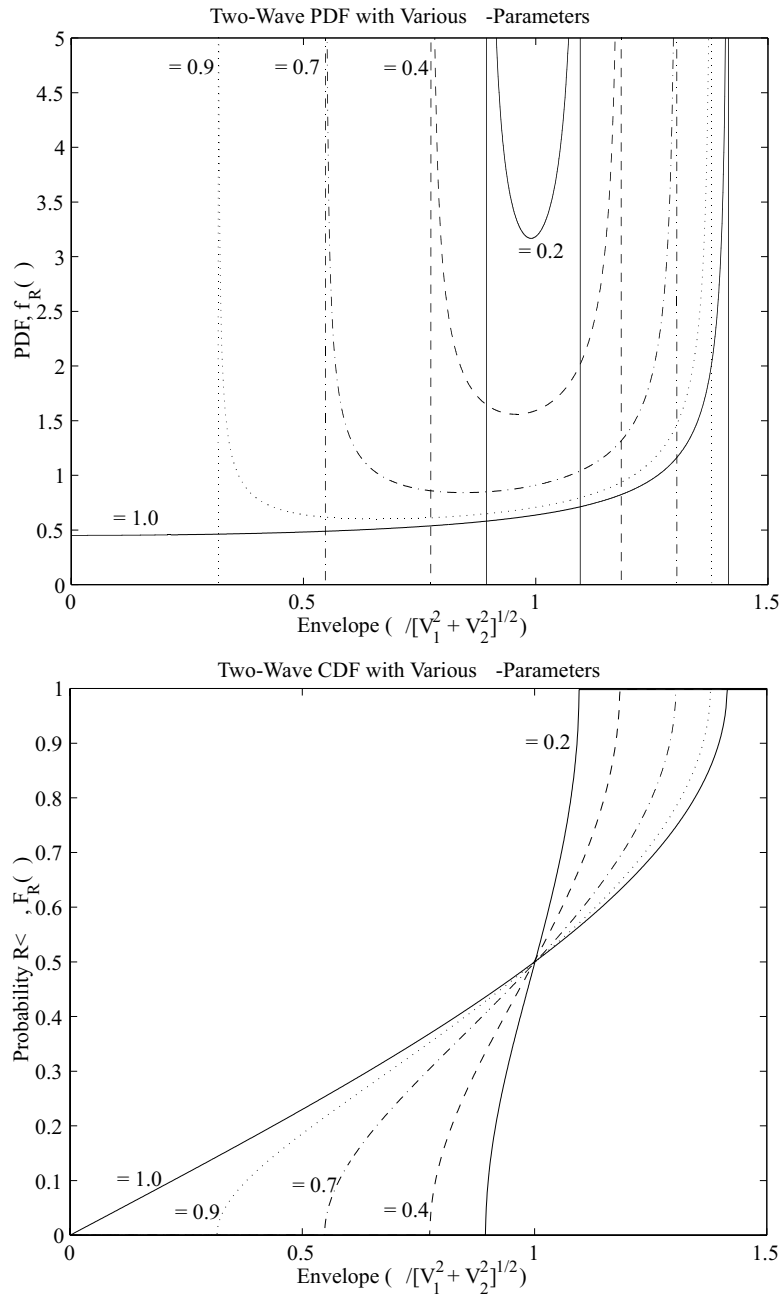
Two-Wave PDF with Various -Parameters

Two-Wave CDF with Various -Parameters

Figure 5.3 Two-wave PDF and CDF with varying Δ [Dur02].

[Nic20] and given below:

$$
f_R(\rho) = \begin{cases} 0, & \rho < \rho_{\min} \text{ or } \rho > \rho_{\max} \\[2ex] \frac{\rho^{\frac{1}{2}}}{\pi^2 \sqrt{V_1 V_2 V_3}} \mathrm{K}\left[\frac{\Delta_\rho^2}{V_1 V_2 V_3 \rho}\right], & \Delta_\rho^2 < V_1 V_2 V_3 \rho \\[2ex] \frac{r}{\pi^2 \Delta_\rho} \mathrm{K}\left[\frac{V_1 V_2 V_3 \rho}{\Delta_\rho^2}\right], & \Delta_\rho^2 > V_1 V_2 V_3 \rho \end{cases} \tag{5.3.4}
$$

The function $\mathrm{K}(\cdot)$ is an elliptic integral of the first kind. Note that Δ_ρ in Equation (5.3.4) is a function of ρ. Here we have used the subscript ρ, which is appended to Nicholson's notation to avoid any confusion between this parameter and the Δ-parameter used to describe the two-wave PDF. The values $\rho_{\min}$ and $\rho_{\max}$ define the interval over which the integration of Equation (5.2.13) and subsequently the PDF is nonzero. They are given by

$$
\rho_{\max} = V_1 + V_2 + V_3 \qquad \rho_{\min} = \max[2\max(V_1, V_2, V_3) - V_1 - V_2 - V_3, 0] \tag{5.3.5}
$$

The expressions in Equation (5.3.5) have an appealing geometric interpretation: The three-wave PDF is 0 for all ρ such that four line segments of lengths ρ, V_1, V_2, and V_3 are incapable of forming a quadrilateral [Nic20]. An IQ sketch of three-wave envelope fading was the example shown in Figure 5.1.

As one might expect, the behavior of the three-wave PDF is varied and complicated. Figure 5.4 plots just a few examples of the PDF and corresponding CDF. A comparison of the three-wave CDFs of Figure 5.4 and the two-wave CDFs of Figure 5.3 provides insight into the difference between specular and nonspecular power. Unlike the two-wave case, the different plots of the three-wave CDF are much more similar to one another. This similarity is due to the central limit theorem: The addition of another constant-amplitude wave to two-wave propagation makes the *total* multipath power more nonspecular. Despite the complex shape of the CDF, the general cases of three-wave propagation begin to approach the CDF for purely nonspecular power. Thus, even if it were possible to analytically calculate a "four-wave PDF," its usefulness would be limited, since the most general cases will appear to be even more Rayleigh-distributed than the three-wave PDF.

5.3.4   The Rayleigh PDF

The Rayleigh PDF assumes that *all* multipath power is nonspecular and occurs from the integration of Equation (5.2.13) under the condition $N = 0$ and nonzero P_{dif}. This definite integral is a standard result and produces the following PDF [Gra94, p. 738]:

$$
f_R(\rho) = \frac{2\rho}{P_{\mathrm{dif}}} \exp\left(\frac{-\rho^2}{P_{\mathrm{dif}}}\right), \quad \rho \geq 0 \tag{5.3.6}
$$

This result was derived as Equation (5.2.11). Unlike the purely specular wave PDFs, the Rayleigh PDF is nonzero over the entire range of $0 \leq \rho < \infty$. The Rayleigh
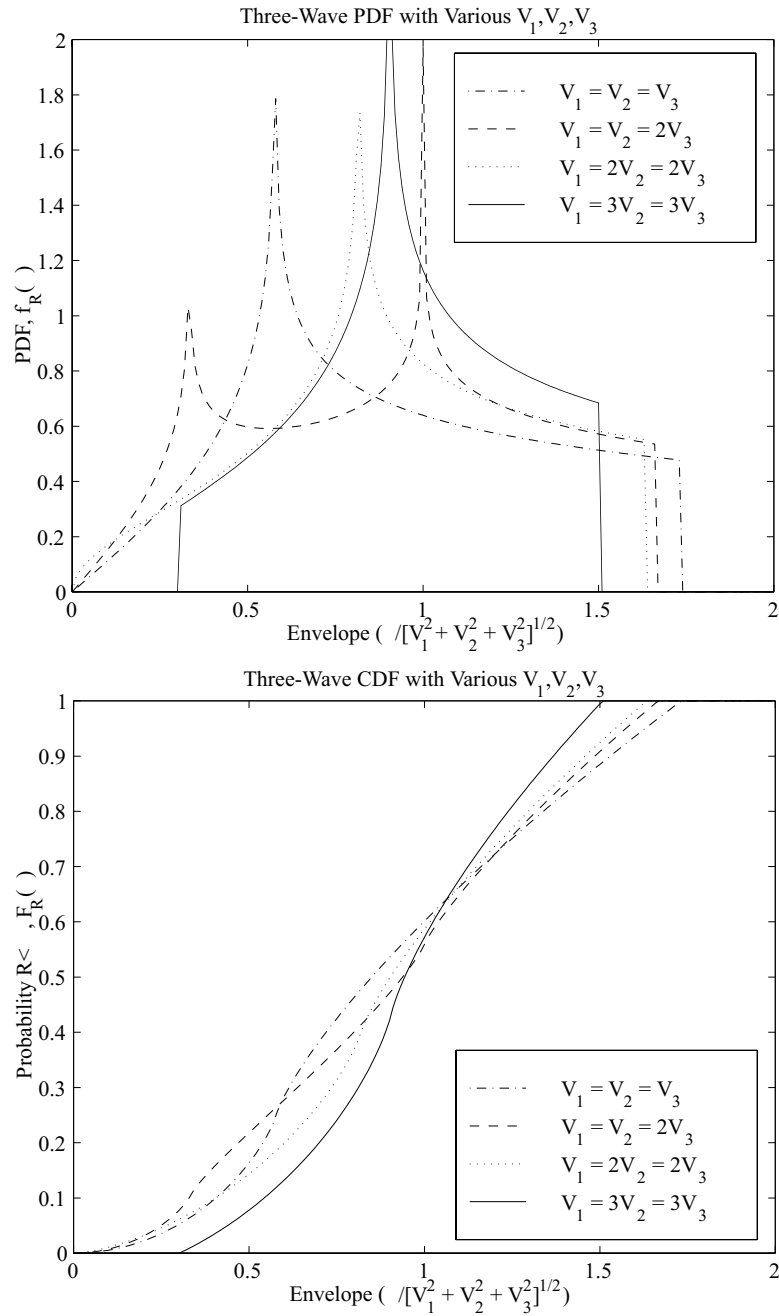
Three-Wave PDF with Various V_1, V_2, V_3

Three-Wave CDF with Various V_1, V_2, V_3

Figure 5.4 Three-wave CDF and PDF for four cases [Dur02].

PDF has been used extensively to describe narrowband local area fading for mobile radio receivers [Par92], [Reu74], [Jak74]. An IQ sketch of the Rayleigh PDF is shown in Figure 5.5.
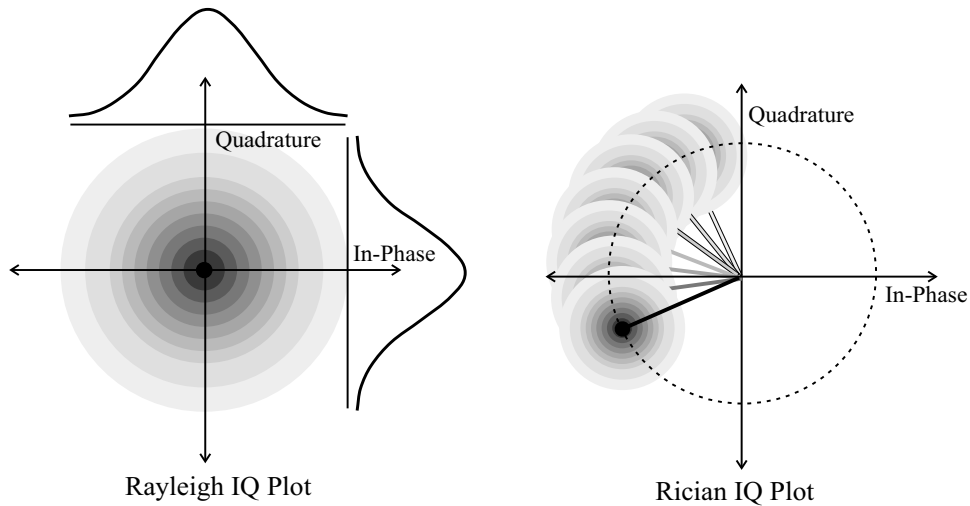

Rayleigh IQ Plot   Rician IQ Plot

Figure 5.5 IQ coordinates with identical, independent Gaussian distributions produce a Rayleigh distribution (left), and adding a specular component produces a Rician distribution (right).

The Rayleigh distribution is the most popular distribution for calculating *fade margins* in radio links for wireless local area networks, cellular phones, and other mobile radio applications. A fade margin is the difference, usually in dB, between the average local area power and the minimum power level for reliable communications. For example, even on the fringe of a coverage area, a wireless engineer plans for an average local area power that is 14 dB to 18 dB higher than the minimum power required for maintaining an acceptable signal-to-noise+interference ratio. Without this extra margin, the channel will fade and create numerous *outages* (i.e., losses of data or service). Example 5.2 illustrates one type of outage calculation.

Example 5.2: Prediction of Link Outage

Problem: An indoor wireless link sends packet data through a Rayleigh fading radio channel. If the link suffers a signal strength fade of more than 10 dB with respect to the average power, packets begin to drop and data is lost. Given this information, about what percentage of data packets are dropped?

Solution: If the average power of a Rayleigh fading radio link is P_{dif}, then a 10 dB fade corresponds to a power of $0.1P_{\text{dif}}$ or, equivalently, a drop of $0.3162\sqrt{P_{\text{dif}}}$ in envelope. To calculate the probability of a Rayleigh channel

dropping below this threshold, we setup and evaluate the following integral:

$$
\begin{aligned}
\Pr[0 \leq R < 0.3162\sqrt{P_{\text{dif}}}] &= \int\limits_{0}^{0.3162\sqrt{P_{\text{dif}}}} \frac{2\rho}{P_{\text{dif}}} \exp\left(\frac{-\rho^2}{P_{\text{dif}}}\right) d\rho \\
&= -\exp\left(\frac{-\rho^2}{P_{\text{dif}}}\right)\Big|_{0}^{\rho=0.3162\sqrt{P_{\text{dif}}}} \\
&= 0.0952
\end{aligned}
$$

If we assume that fades are slow with respect to data packet length, we can estimate that 9.5% of the packets will be dropped.

5.3.5   The Rician PDF

The Rician PDF describes the fading of nonspecular power in the presence of a dominant, nonfluctuating multipath component [Reu74], [Ric48]. The analytical expression for the Rician distribution results from the integration of Equation (5.2.13) under the condition $N = 1$ and nonzero P_{dif}. After applying a well-understood definite integral relationship [Gra94, p. 739], the resulting PDF is

$$
f_R(\rho) = \frac{2\rho}{P_{\text{dif}}} \exp\left(\frac{-\rho^2 - V_1^2}{P_{\text{dif}}}\right) \text{I}_0\left(\frac{2\rho V_1}{P_{\text{dif}}}\right), \quad \rho \geq 0 \tag{5.3.7}
$$

where $\text{I}_0(\cdot)$ is a zero-order modified Bessel function. An IQ sketch of the Rician PDF is shown in Figure 5.5.

Figure 5.6 shows several different kinds of Rician PDFs and CDFs. The plots are labeled using a Rician K factor, which is the ratio of the power of the dominant multipath component to the power of the remaining nonspecular multipath:

$$
K = \frac{\text{Specular Power}}{\text{Nonspecular Power}} = \frac{V_1^2}{P_{\text{dif}}} \tag{5.3.8}
$$

In the literature, the parameter K is often given as a dB value, which is $10\log_{10}$ of the quantity in Equation (5.3.8). Notice from Figure 5.6 that $K = -\infty$ dB corresponds to the Rayleigh PDF and the complete disappearance of the specular power.

Note: A Useful Approximation

As the Rician K-factor becomes large ($K \gg 1$), it is possible to approximate the Rician distribution with a Gaussian PDF of the following form:

$$
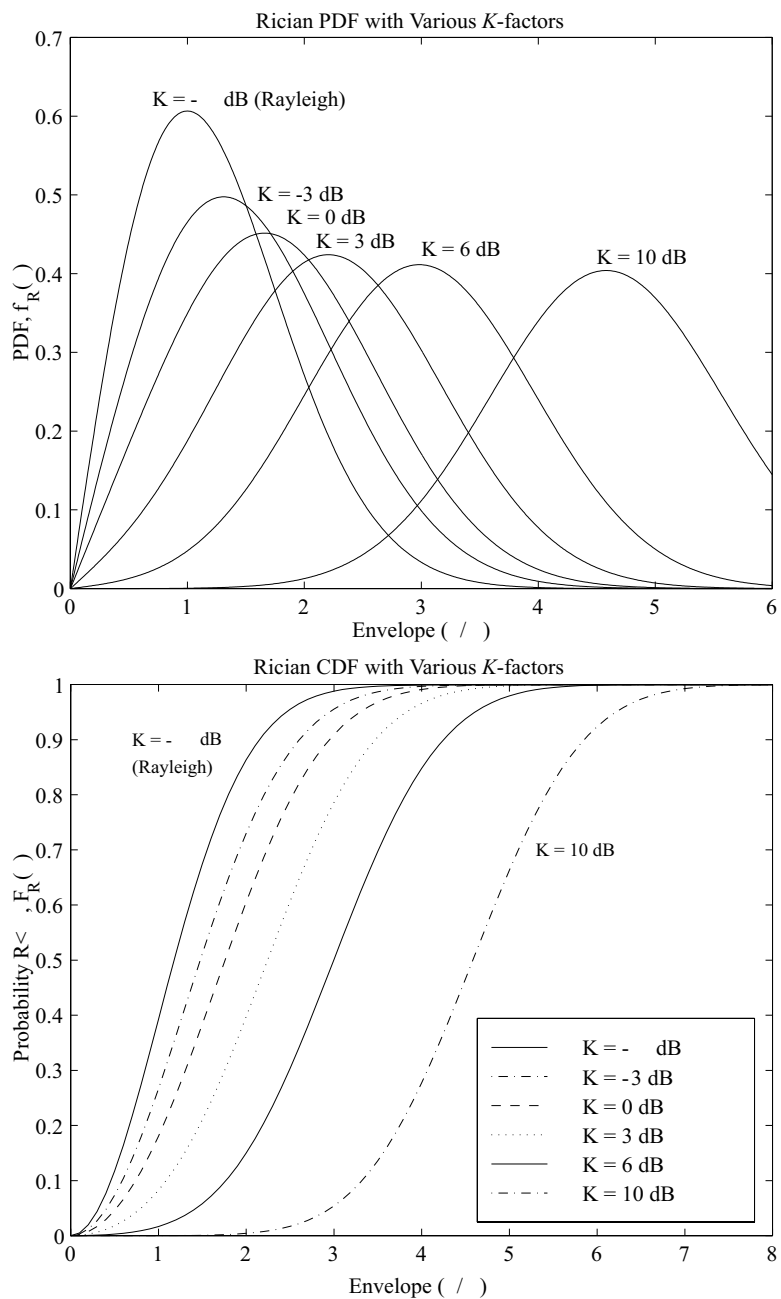f_R(\rho) = \frac{1}{\sqrt{\pi P_{\text{dif}}}} \exp\left(-\frac{(\rho - V_1)^2}{P_{\text{dif}}}\right)
$$

Rician PDF with Various *K*-factors

Rician CDF with Various *K*-factors

Figure 5.6 Rician PDF and CDF as the dominant multipath component increases ($\sigma = \sqrt{P_{\mathrm{dif}}/2}$) [Dur02].

Note: Rice or Nakagami

The Rician distribution is also called the *Rice-Nakagami* distribution in the literature to recognize the result that was independently formulated by outstanding Japanese researcher M. Nakagami. The term *Rician* is used in this work not to diminish Nakagami's contribution, but to avoid confusion with another popular PDF in radio channel modeling that bears his name: the *Nakagami-m* distribution [Nak60]. This distribution was originally formulated for characterizing temporal fading measurements from upper-atmosphere propagation but has been applied liberally to the small-scale fading of terrestrial wireless systems as well [Cou98a], [Yac00].

5.4 Two-Wave with Diffuse Power PDF

If Equation (5.2.13) is evaluated with $N = 2$ and nonzero P_{dif}, then the two-wave with diffuse power (TWDP) PDF results [Esp73], [Dur02]. Such a distribution, while difficult to model analytically, provides the greatest wealth of fading behavior for an I-SLAC model.

5.4.1 Approximate Representation

We will use parameters similar to the physical Rician K-parameter of Equation (5.3.8) and the two-wave Δ-parameter of Equation (5.3.3) to classify the shape of the TWDP PDF:

$$K = \frac{V_1^2 + V_2^2}{P_{\text{dif}}} \qquad \Delta = \frac{2V_1 V_2}{V_1^2 + V_2^2} \tag{5.4.1}$$

There is no exact closed-form equation for TWDP fading, but this section presents a family of closed-form PDFs that closely approximate the behavior of the exact TWDP PDF.

An IQ sketch of TWDP fading is shown in Figure 5.7. One common approximation to the TWDP PDF is presented in [Dur02]:

$$f_R(\rho) = \frac{2\rho}{P_{\text{dif}}} \exp\left(\frac{-\rho^2}{P_{\text{dif}}} - K\right) \sum_{i=1}^{M} a_i \mathrm{D}\left(\frac{\rho}{\sqrt{P_{\text{dif}}/2}}; K, \Delta \cos\frac{\pi(i-1)}{2M-1}\right) \tag{5.4.2}$$

where

$$\mathrm{D}\left(x; K, \alpha\right) = \frac{1}{2} \exp(\alpha K)\mathrm{I}_0\left(x\sqrt{2K(1-\alpha)}\right) + \frac{1}{2} \exp(-\alpha K)\mathrm{I}_0\left(x\sqrt{2K(1+\alpha)}\right).$$

The value M in the summation is the *order* of the approximate TWDP PDF. By increasing the order in Equation (5.4.2), the approximate PDF becomes a more accurate representation of the true TWDP PDF. However, using the first few orders ($M = 1$ through 5) yields accurate representations *over the most useful range of K and Δ parameters*. Table 5.2 records the exact $\{a_i\}$ coefficients for the first five orders of Equation (5.4.2).
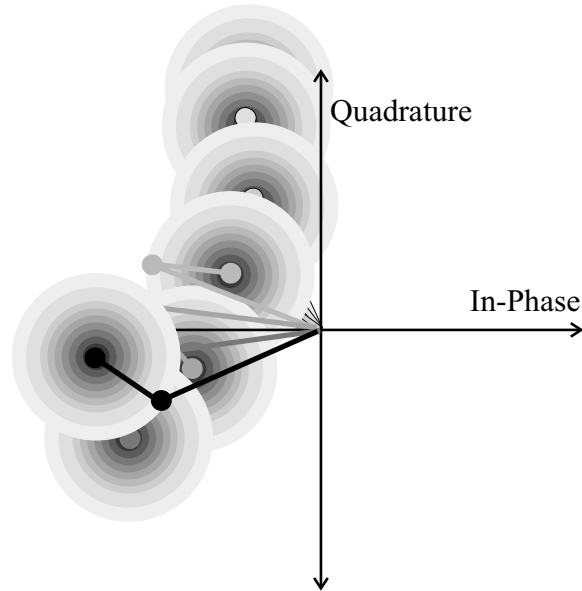
Figure 5.7   A diffuse, Rayleigh component added to two randomly phased specular waves to produce a TWDP distribution.

Table 5.2   Exact Coefficients for the First Five Orders of the Approximate TWDP Fading PDF

ORDER	a_1	a_2	a_3	a_4	a_5
1	1				
2	$\frac{1}{4}$	$\frac{3}{4}$			
3	$\frac{19}{144}$	$\frac{25}{48}$	$\frac{25}{72}$		
4	$\frac{751}{8640}$	$\frac{3577}{8640}$	$\frac{49}{320}$	$\frac{2989}{8640}$	
5	$\frac{2857}{44800}$	$\frac{15741}{44800}$	$\frac{27}{1120}$	$\frac{1209}{2800}$	$\frac{2889}{22400}$

The product of the parameters K and Δ determines which order of Equation (5.4.2) should be used when representing TWDP fading. As the product of these two parameters increases, a higher order approximation is needed to model the TWDP PDF accurately. As a general rule of thumb, the minimum order is

$$\text{Order } (M) = \left\lceil \frac{1}{2} K \Delta \right\rceil \tag{5.4.3}$$

where $\lceil \cdot \rceil$ is the ceiling function (round up). Equation (5.4.3) is based on a graphical

comparison between the approximate analytical functions and the true, numerical solution of the TWDP PDF. The approximate PDF will deviate from the exact TWDP PDF only if the specular power is much larger than the nonspecular power (large K value) *and* if the amplitudes of the specular voltage components are relatively equal in magnitude (Δ approaches 1).

Example 5.3: Order-2 Approximate TWDP PDF

Problem: Using Table 5.2 and Equation (5.4.2), calculate the order-2 approximate TWDP PDF.

Solution: Plugging the coefficients a_1 and a_2 into Equation (5.4.2) produces

$$f_R(\rho) = \frac{2\rho}{P_{\mathrm{dif}}} \exp\left(\frac{-\rho^2}{P_{\mathrm{dif}}} - K\right)\left[\frac{1}{4}\mathrm{D}\left(\frac{\rho}{\sqrt{P_{\mathrm{dif}}/2}}; K, \Delta\right) + \frac{3}{4}\mathrm{D}\left(\frac{\rho}{\sqrt{P_{\mathrm{dif}}/2}}; K, \frac{\Delta}{2}\right)\right]$$

which, in this form, is not much more complicated than a Rician PDF.

Despite being an approximate result, the family of PDFs in Equation (5.4.2) have a number of extraordinary characteristics that are independent of order, M, and parameters, K and Δ:

- *They are mathematically exact PDFs.* They integrate to 1 over the range $0 \leq \rho < \infty$.

- *They are accurate over their upper and lower tails.* These regions are important for modeling noise-limited or interference-limited mobile communication systems [Cou98b].

- *They all exactly preserve the second moment of the true PDF.* The second moment is the most important moment to preserve, since it physically represents the average local area power [Rap02a].

- *They can be entirely described with three physically intuitive parameters.* The physical parameters P_{dif}, K, and Δ - as defined in this book - have straightforward physical definitions.

- *They exhibit the proper limiting behavior.* All of the PDFs contain, as a special case of $\Delta = 0$, the exact Rician PDF and, as a special case of $K = 0$, the exact Rayleigh PDF.

Accurate analytical representation of these PDFs reveals interesting behavior in fading channels that goes unnoticed using Rician PDFs, which are capable of modeling the envelope fading of diffuse power in the presence of only *one* specular component.

It should be noted that there are many interesting ways to approximate the TWDP PDF and other nonanalytic forms of Equation (5.2.13) (see the work by Esposita and Wilson in [Esp73] and Abdi et al. in [Abd00]).

5.4.2 Graphical Analysis

Figures 5.8 through 5.11 plot a series of PDFs and CDFs for TWDP fading. As shown by Figure 5.8, there is little difference between the Rician PDF and the TWDP PDF when K is less than 3 dB. The difference gradually becomes more pronounced as K increases, particularly when the specular power is divided equally between the two discrete components ($\Delta = 1$). The $K = 10$ dB graph of Figure 5.11 illustrates these distortions most dramatically. In fact, as the product of parameters K and Δ becomes large, the graph of the PDF becomes bimodal, exhibiting two maxima.

5.4.3 Rayleigh and Rician Approximations

For the limiting parameter cases of Table 5.3, the exact TWDP PDF contains the Rayleigh, Rician, one-wave, and two-wave PDFs. This demonstrates the generality of the exact and approximate TWDP PDFs. It also shows the utility of the three-wave PDF, since it is the only analytical expression in Table 5.1 that is not a general case of the TWDP PDF.

Table 5.3 The TWDP PDF Contains the Rayleigh, Rician, One-Wave, and Two-Wave PDFs as Special Cases

Parameter Value		Type of Fading
$K = 0$	$-$	Rayleigh
$K > 0$	$\Delta = 0$	Rician
$K \to \infty$	$\Delta = 0$	One-Wave
$K \to \infty$	$\Delta > 0$	Two-Wave

Since the Rician and Rayleigh PDFs are special cases of the TWDP PDF, it is useful to know the range of parameters over which TWDP fading may be approximated by these simpler distributions. An inspection of the graphs of Figure 5.8 through Figure 5.11 reveals the range of K and Δ over which a Rician PDF approximates a TWDP PDF. In general, the TWDP PDF resembles a Rician PDF in shape for $K\Delta < 2$. Under this condition, the smallest of the two specular components may be grouped with the nonspecular power so that only one large specular component remains. After computing a Rician K-factor for this new grouping, the resulting Rician PDF will approximately describe the envelope of the TWDP fading.

TWDP fading may be further approximated by a Rayleigh PDF if, in addition to the above-mentioned criterion, the power of the largest specular component is less than the power of the smaller specular component *plus* the average nonspecular power:

$$\max(V_1^2, V_2^2) \; < \; \min(V_1^2, V_2^2) + P_{\text{dif}}$$

$$\frac{1}{2} + \frac{1}{2}\sqrt{1 - \Delta^2} \; < \; \frac{1}{2} - \frac{1}{2}\sqrt{1 - \Delta^2} + \frac{1}{K + 1} \qquad (5.4.4)$$
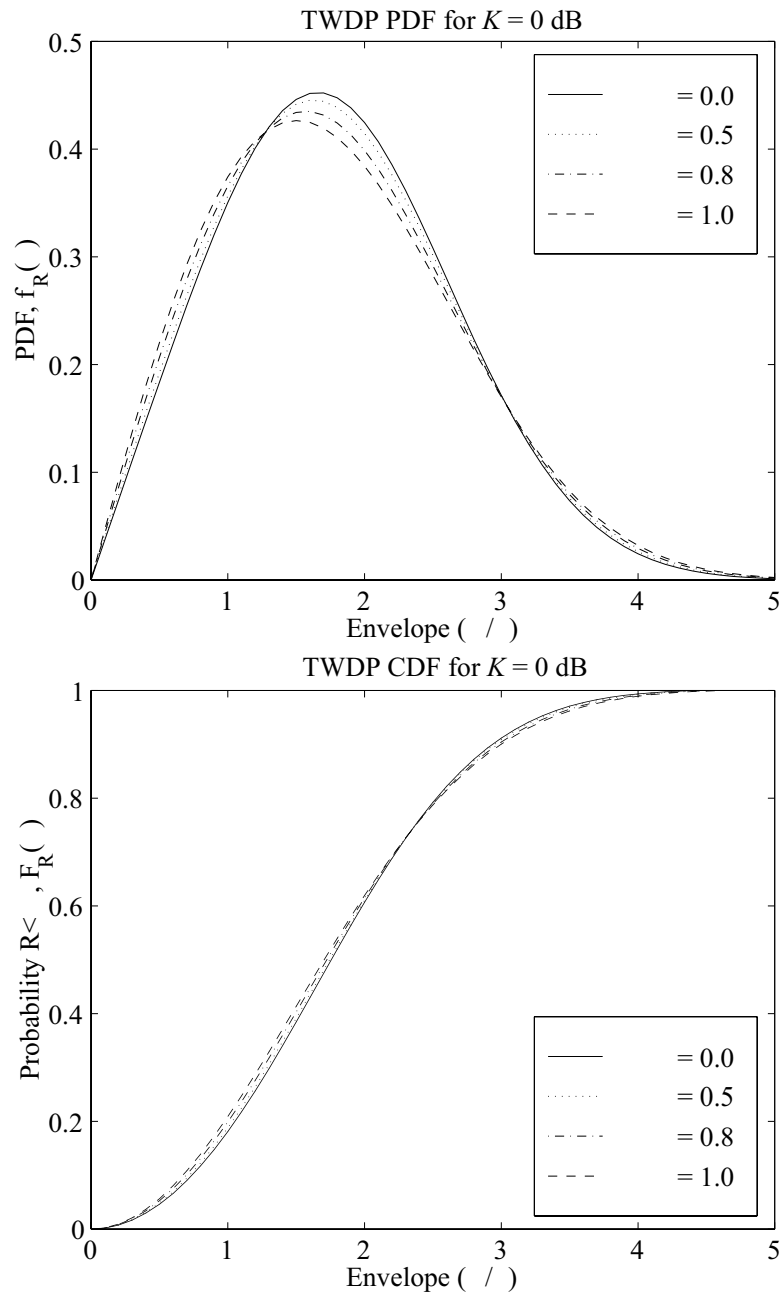
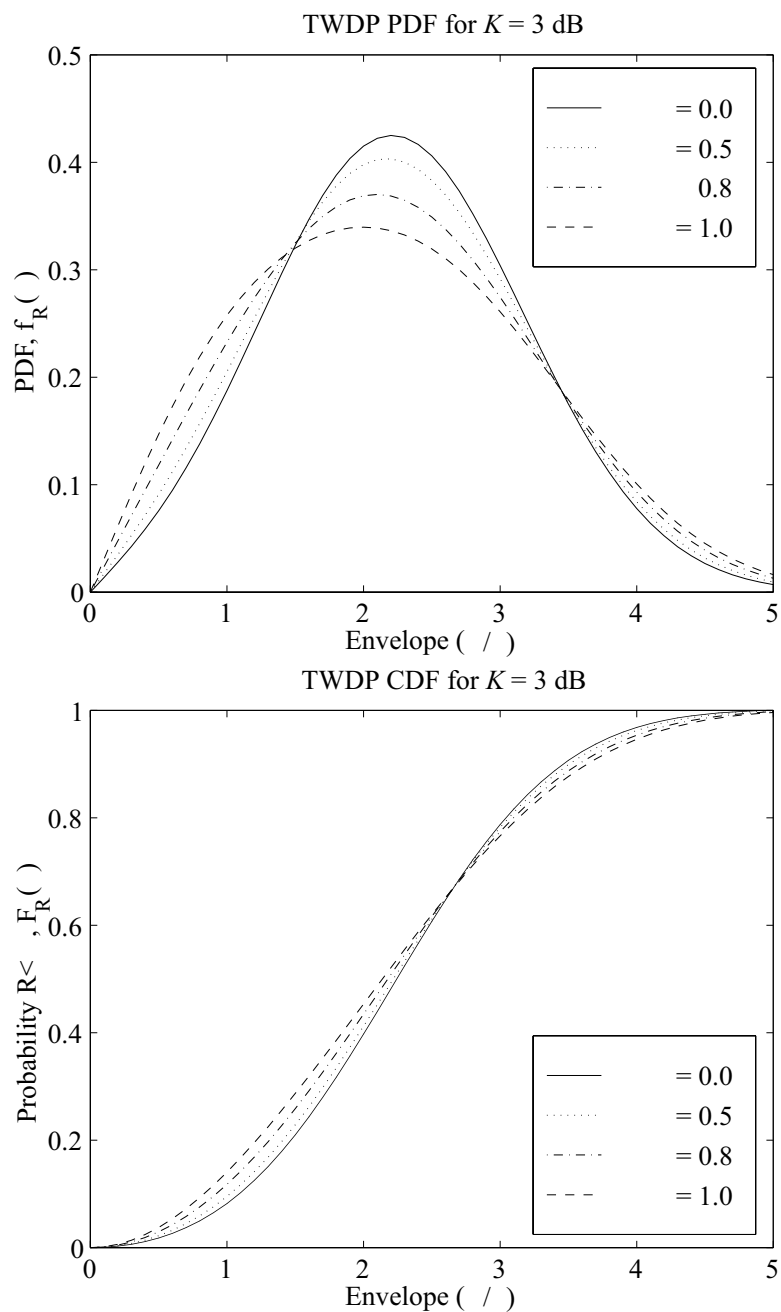**Figure 5.8** TWDP PDF and CDF for $K = 0$ dB [Dur02] $(\sigma = \sqrt{P_{\text{dif}}/2})$.

TWDP PDF for $K = 3$ dB

TWDP CDF for $K = 3$ dB

Figure 5.9 TWDP PDF and CDF for $K = 3$ dB [Dur02] ($\sigma = \sqrt{P_{\mathrm{dif}}/2}$).

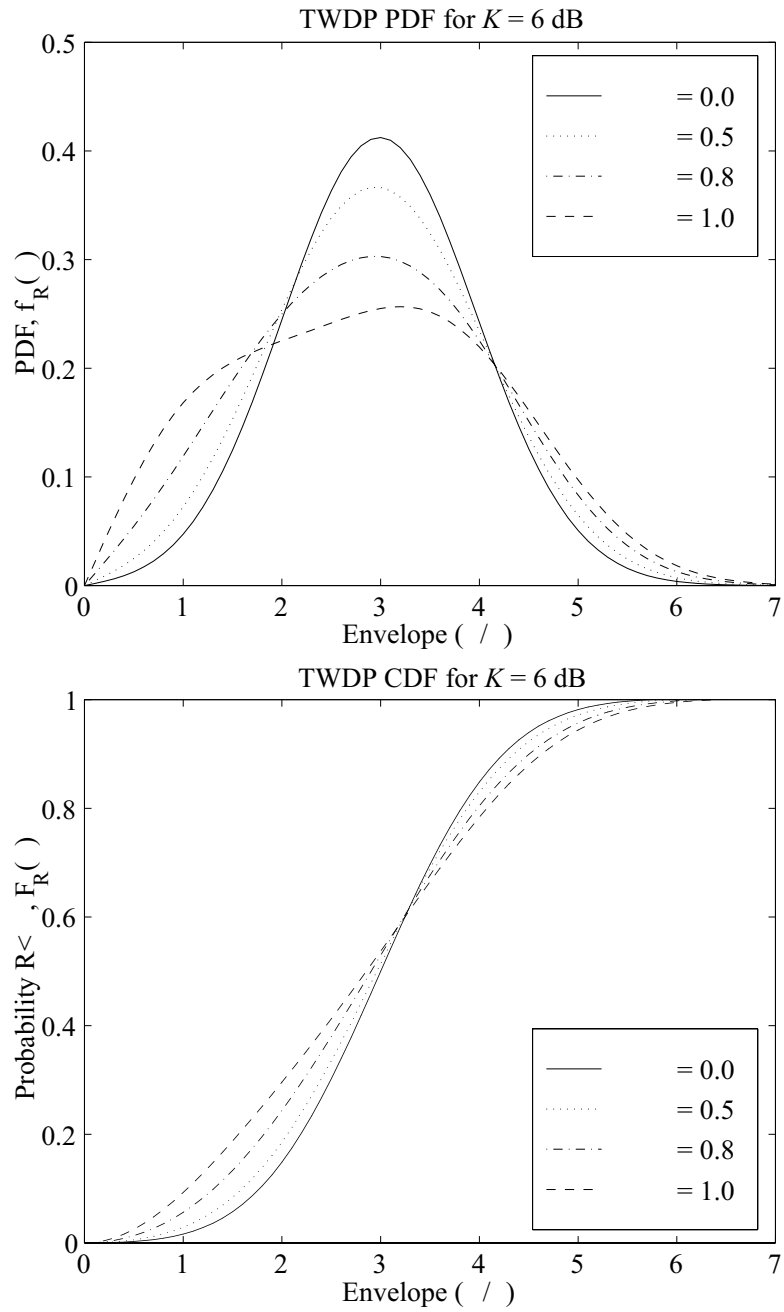**Figure 5.10** TWDP PDF and CDF for $K = 6$ dB [Dur02] ($\sigma = \sqrt{P_{\text{dif}}/2}$).

TWDP PDF for $K = 10$ dB
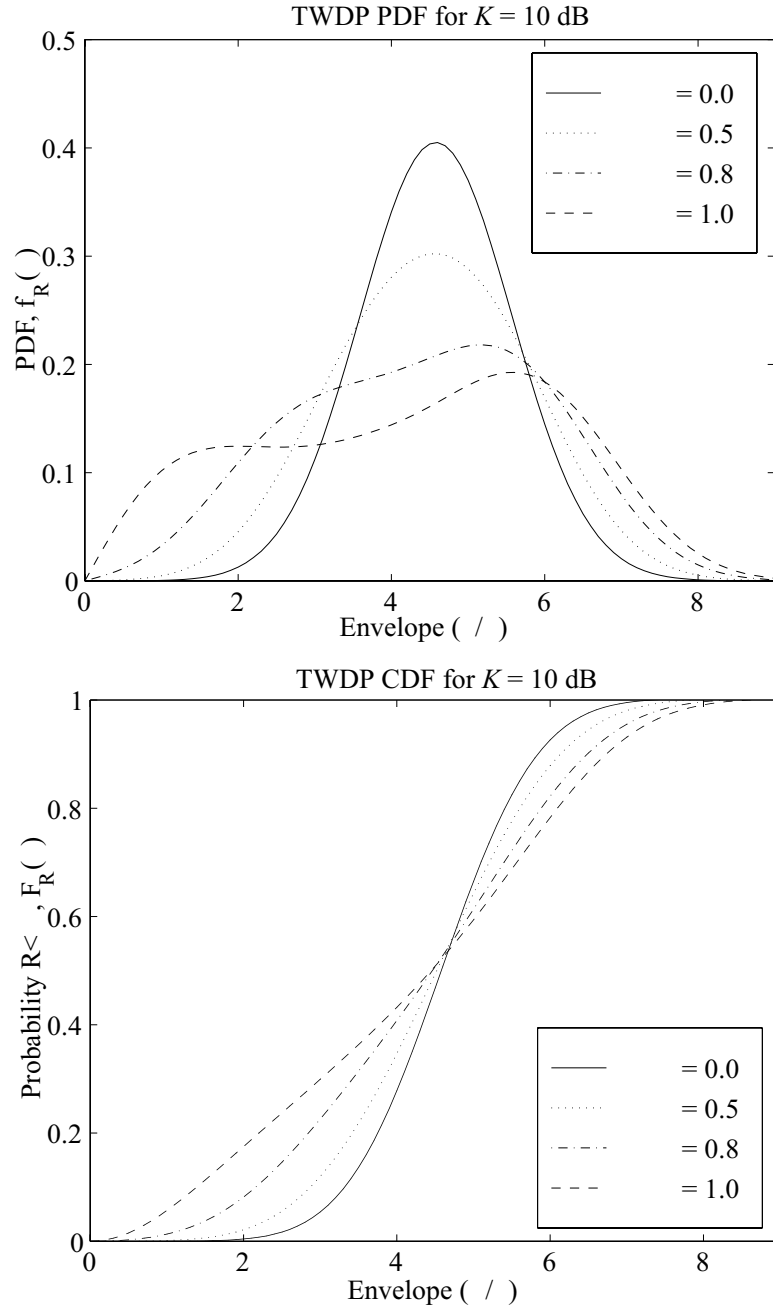

TWDP CDF for $K = 10$ dB

Figure 5.11 TWDP PDF and CDF for $K = 10$ dB [Dur02] ($\sigma = \sqrt{P_{\mathrm{dif}}/2}$).

This condition derives from Figure 5.6, which shows that Rician PDFs resemble the shapes of Rayleigh PDFs (after scaling) for a Rician K-factor less than 0 dB. Under this condition, the entire sum of voltage components may be treated together as diffuse, nonspecular power, despite the presence of two specular components.

The Rician and Rayleigh approximation conditions, therefore, are best summarized in terms of the TWDP K and Δ parameters by the following:

$$\text{Rician Condition:} \quad K < \frac{2}{\Delta} \tag{5.4.5}$$

$$\text{Rayleigh Condition:} \quad K < \min\left(\frac{2}{\Delta}, \frac{1}{\sqrt{1-\Delta^2}} - 1\right) \tag{5.4.6}$$

These conditions show the parameter range over which a TWDP PDF may be approximated by an analytically simpler Rician or Rayleigh PDF. If these conditions are not met, then the only recourse is to use Equation (5.4.2) or some other evaluation of Equation (5.2.13) for $N = 2$ and nonzero P_{dif}.

Table 5.4 shows three examples of TWDP fading and determines the simplest approximate PDF that describes the voltage envelope of each. Case A in Table 5.4 satisfies the Rayleigh condition of Equation (5.4.6). Case B, on the other hand, satisfies only the Rician condition of Equation (5.4.5). Case C satisfies neither condition and may not be approximated by a Rayleigh or Rician PDF. Note how the subtle changes in voltage amplitudes between the three cases drastically affects the overall shape and calculation of the PDF, emphasizing the need for careful and accurate representation of TWDP PDFs. See Example 5.4 for another example of finding the optimum PDF representation.

Table 5.4 Three Examples of TWDP Fading That May Simplify to Rayleigh or Rician PDFs

	EXAMPLE TWDP VOLTAGE VALUES			Parameters		Simplest
Case	1st Specular Voltage (V_1)	2nd Specular Voltage (V_2)	Diffuse RMS Voltage ($\sqrt{P_{\text{dif}}}$)	K	Δ	PDF
A	2 μV	2 μV	3 μV	0.89	1.0	Rayleigh
B	4 μV	2 μV	3 μV	2.22	0.8	Rician
C	4 μV	4 μV	3 μV	3.56	1.0	TWDP

Example 5.4: PDF Grouping

Problem: It is known that an I-SLAC model is composed of three multipath waves with voltage amplitudes 4 μV, 3 μV, and 2 μV and a diffuse, nonspecular component with $P_{\text{dif}} = (1\mu V)^2$. Find the simplest analytical representation, if any, of this envelope PDF.

Solution: Perform the following steps to ascertain the best PDF:

1. The initial grouping of voltages is $[V_1 = 4, V_2 = 3, V_3 = 2, P_{\text{dif}} = 1]$ (units dropped for simplicity).

2. There is diffuse power ($P_{\text{dif}} \neq 0$) and there are more than two specular components ($N = 3$), so all but the two largest specular components must be grouped with the nonspecular component. The new grouping is $[V_1 = 4, V_2 = 3, P_{\text{dif}} = 5]$.

3. The TWDP factors for this distribution are $K = 5$ and $\Delta = 0.96$. This TWDP distribution is too complicated to simplify to a Rayleigh distribution ($K > 1$) or a Rician distribution ($K\Delta > 1$), but can be approximated accurately by Equation (5.4.2) ($K\Delta < 10$).

4. The value of $\left\lceil \frac{K\Delta}{2} \right\rceil$ is 3, so an order-3 approximation of Equation (5.4.2) should be used to represent the PDF.

5.4.4   TWDP PDF Applications

The TWDP PDF and its approximations are important for characterizing fading in a variety of propagation scenarios. Small-scale fading is characterized by the TWDP PDF whenever the received signal contains two strong, specular multipath waves. While this may occur for typical narrowband receiver operation, directional antennas and wideband signals increase the likelihood of TWDP small-scale fading.

The use of directive antennas or arrays at a receiver, for example, amplifies several of the strongest multipath waves that arrive in one particular direction while attenuating the remaining waves [God97], [Win98]. This effectively increases the ratio of specular to nonspecular received power, turning a Rayleigh or Rician fading channel into a TWDP fading channel.

Wideband signal fading will likely exhibit TWDP fading characteristics for similar reasons. A wideband receiver has the ability to reject multipath components that arrive with largely different propagation time delays [Rap02a], [Bra91]. This property of a wideband receiver separates specular multipath components from other nonspecular multipath waves. Under these circumstances, the ratio of specular to nonspecular received power increases for a given propagation delay and a TWDP fading channel may result.

5.4.5   Closing Remarks on TWDP Fading

Beyond the TWDP PDF, a three-wave with diffuse power (3WDP) PDF is the next logical step. The value of such an analytically difficult PDF, however, is questionable. Much like the previously discussed four-wave PDF, the central-limit theorem would begin to dominate the behavior of an I-SLAC model, making it difficult to distinguish between the different cases of a 3WDP PDF. For example, a 3WDP PDF may be approximated by the TWDP PDF if the smallest of the three specular voltage components is grouped with the nonspecular power. This approximation would fail only if the nonspecular power were small compared to the third smallest

specular component - yet such a situation implies that the nonspecular power is so small that it could be ignored: A 3WDP PDF could then be approximated by the three-wave PDF. Therefore, it is safe to say that the analytical expressions of Equation (5.4.2) and Table 5.1 provide a near-complete description of the possible envelope fading of complex voltages in an I-SLAC model.

5.5   Chapter Summary

In a randomly varying small-scale channel, the distribution of received signal power or envelope dramatically affects the performance of a receiver. These fluctuations are best described using a PDF, which characterizes all of the first-order statistics of a channel. The following key points summarize the first-order analysis described in this chapter:

- ■ Mean received power is one of the most fundamental first-order statistics in channel modeling and measurement.

  - ▷ For a U-SLAC model, the mean power of the channel is equal to the sum of the powers carried by individual multipath waves.
  - ▷ An I-SLAC model is strict-sense stationary.
  - ▷ A U-SLAC model is ergodic if its scattering is heterogeneous.
  - ▷ For a U-SLAC model with heterogeneous scattering, spatial averaging and frequency averaging produce identical results for mean received power.

- ■ The canonical PDF generator of Equation (5.2.13) describes the distribution of received envelope voltages for I-SLAC models.

  - ▷ The generator is based on the reduced wave grouping and uses a characteristic function approach.
  - ▷ There are five closed-form solutions to the PDF generator.
  - ▷ The simplest solutions have become popular in wireless engineering.

- ■ The two-wave with diffuse power (TWDP) PDF models the most general type of fading behavior.

  - ▷ This PDF has no closed-form solution.
  - ▷ There are several techniques for approximating the TWDP PDF.
  - ▷ The TWDP PDF contains Rayleigh, Rician, one-wave, and two-wave PDFs as special cases.
  - ▷ TWDP behavior can deviate substantially from Rayleigh or Rician PDFs.

Envelope PDF calculation completely characterizes the first-order power statistics of a random radio channel. While useful, first-order statistics do not provide any information as to how processes develop as a function of frequency and space. To

understand the space-varying characteristics of random channels, we will further develop our analysis of the 3D spatial channel and introduce the concept of multipath *angle spectrum*. This is the subject of Chapter 6.

PROBLEMS

1. The following statistic, χ, is used to describe a frequency-varying I-SLAC model, $\tilde{h}(f)$:
$$\chi(f_1, f_2, f_3) = \mathrm{E}\left\{\tilde{h}(f_1)\tilde{h}^*(f_2)\tilde{h}(f_3)\right\}$$
Demonstrate how it is possible to simplify the number of dependencies in this statistic.

2. You decide to measure local area power using two techniques. First, you measure the spatial average of a narrowband channel, $\tilde{h}(\vec{r})$. Then, you measure the frequency average of a fixed channel, $\tilde{h}(f)$. Explain a possible physical interpretation for the multipath waves if the two averages do not agree.

3. Why are the following functions invalid for use as an envelope PDF?

    a. $f_R(\rho) = \frac{1}{\sigma\sqrt{2\pi}}\exp\left(-\frac{\rho^2}{2\sigma^2}\right)$

    b. $f_R(\rho) = \mathrm{u}(\rho - 1) - \mathrm{u}(\rho - 3)$

    c. $f_R(\rho) = \mathrm{sn}(\rho - 3)\mathrm{u}(\rho)$

    d. $f_R(\rho) = \mathrm{sn}^2(\rho)\mathrm{u}(\rho)$

4. Transform the following envelope PDFs into power PDFs based on the relationship $p = \rho^2$:

    a. Weibull PDF: $f_R(\rho) = a\exp\left(-ap\right)\mathrm{u}(p), \quad a > 0$

    b. Half-Gaussian PDF: $f_R(\rho) = \frac{1}{\sigma}\sqrt{\frac{2}{\pi}}\exp\left(-\frac{\rho^2}{2\sigma^2}\right)\mathrm{u}(\rho)$

    c. Two-Wave PDF: $f_R(\rho) = \frac{2\rho}{\pi\sqrt{4V_1^2 V_2^2 - (V_1^2 + V_2^2 - \rho^2)^2}}$, for $|V_1 - V_2| \leq \rho \leq V_1 + V_2$

    d. Rician PDF: $f_R(\rho) = \frac{2\rho}{P_{\mathrm{dif}}}\exp\left(\frac{-\rho^2 - V_1^2}{P_{\mathrm{dif}}}\right)\mathrm{I}_0\left(\frac{2V_1\rho}{P_{\mathrm{dif}}}\right)\mathrm{u}(\rho)$

    e. Half Sinc-Squared PDF: $f_R(\rho) = 2V_0\mathrm{sn}^2(V_0\rho)\mathrm{u}(\rho)$

5. Transform the following power PDFs into envelope PDFs based on the relationship $p = \rho^2$:
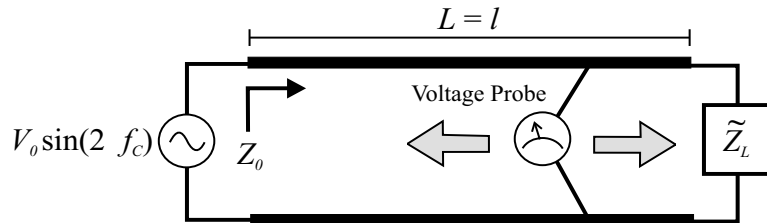
    a. Exponential: $f_P(p) = \frac{1}{P_0}\exp\left(-\frac{p}{P_0}\right)\mathrm{u}(p)$

    b. Half-Gaussian PDF: $f_P(p) = \frac{1}{\sigma}\sqrt{\frac{2}{\pi}}\exp\left(-\frac{p^2}{2\sigma^2}\right)\mathrm{u}(p)$

    c. Triangle PDF: $f_P(p) = 2(1 - p)[\mathrm{u}(p) - \mathrm{u}(p - 1)]$

    d. Half Sinc-Squared PDF: $f_P(p) = 2P_0\mathrm{sn}^2(P_0 p)\mathrm{u}(p)$

6. Recall the transmission line problem from previous engineering courses. A lossless transmission line of length $L = l\lambda$ and real impedance, Z_0, terminates in a complex load with impedance, $\tilde{Z}_L$. This configuration is illustrated below:

The transmission line is very long, and a voltage probe takes measurements at random positions along the length of the line. Find an expression for the envelope PDF measured by the probe in terms of l, Z_0, and $\tilde{Z}_L$.

7. 🖳   Write a computer program to numerically compute any PDF from the I-SLAC PDF generator of Equation (5.2.13). Use this program to graph the PDFs for the following cases:

    a. $N = 4$, $V_1 = V_2 = V_3 = V_4 = 1\text{V}$, $P_{\text{dif}} = 1\text{V}^2$

    b. $N = 4$, $V_1 = V_2 = V_3 = V_4 = 1\text{V}$, $P_{\text{dif}} = 0$

    c. $N = 4$, $V_1 = V_2 = 2V_3 = 2V_4 = 1\text{V}$, $P_{\text{dif}} = 0$

    d. $N = 3$, $V_1 = V_2 = 2V_3 = 1\text{V}$, $P_{\text{dif}} = 1\text{V}^2$

    e. $N = 3$, $V_1 = 2V_2 = 2V_3 = 1\text{V}$, $P_{\text{dif}} = 1\text{V}^2$

8. 🖳   Consider a local area propagation scenario where three equal-amplitude specular waves ($V_1 = V_2 = V_3 = 1\text{V}$) are received in the presence of other diffuse multipath waves with total power P_0. We may can calculate this case by either grouping one of the specular voltages with the diffuse power (a TWDP approximation) or using the full 3WDP representation:

$$\text{TWDP:} \quad \begin{array}{l} V_1 = V_2 = 1\text{V} \\ P_{\text{dif}} = P_0 + 1\text{V}^2 \end{array} \qquad \text{3WDP:} \quad \begin{array}{l} V_1 = V_2 = V_3 = 1\text{V} \\ P_{\text{dif}} = P_0 \end{array}$$

Evaluate and graph both the exact 3WDP and approximate TWDP envelope PDFs for different values of P_0. At which value of P_0 does this approximation fail?

9. Use the Rayleigh PDF to calculate the following information about a Rayleigh fading channel with average power P_{dif}:

    a. What is the mean of the Rayleigh fading envelope?

    b. What is the most likely value of the envelope?

    c. What is the *median* of the envelope? (The median is the voltage, ρ_m, at which $\Pr[R > \rho_m] = \Pr[R < \rho_m] = 0.5$.)

10. Analytically write and solve the generating integral for the Rician PDF. Hint: See Appendix A.4 for formulas that help evaluate this integral.

11. Prove that the following mathematical relationship holds for any positive values of A_i:

$$\int\limits_0^\infty \int\limits_0^\infty x^3 \nu \prod_{i=1}^N J_0(A_i \nu) J_0(\nu x) \, d\nu \, dx = \sum_{i=1}^N A_i^2$$

Hint: Try applying some theorems learned in this chapter before computing any integrals.

12. Prove that the Rician distribution may be approximated as a Gaussian distribution for $K \gg 1$. (See Table A.3 in Appendix A.)

13. Which of the following descriptions of wave groupings will produce envelopes that never fade to zero?

    a. $\{V_i\} = \{4, 3, 2, 1\}$

    b. $\{V_i\} = \{4, 2, 1\}$

    c. $\{V_i\} = \{1, 3, 4, 10, 1\}$

    d. $\{V_i\} = \{200, 1, 1\}$ and $P_{\text{dif}} = 0.1 \text{V}^2$

14. Compute $\mathrm{E}\{P\}$ for the groups of waves in the previous problem.

15. � Assume that N specular waves with equal amplitude are received by an antenna. Test how the exact I-SLAC PDF compares with an approximation of the PDF using the Rayleigh distribution of equal power. Graph the cases for $N = 3, 4, 5, 7, 10, 15,$ and 20.

5.A   Envelope Characteristic Functions

In the study of PDFs, it is convenient to define a characteristic function, which is the Fourier transform of the PDF [Pap91]. The standard mathematical definitions for finding a characteristic function, $\Phi_X(v)$, from a PDF, $f_X(x)$, and vice versa are given below:

$$\Phi_X(v) = \int\limits_{-\infty}^{+\infty} f_X(x)\exp(-jvx)\,dx \tag{5.A.1}$$

$$f_X(x) = \frac{1}{2\pi}\int\limits_{-\infty}^{+\infty} \Phi_X(v)\exp(jvx)\,dv \tag{5.A.2}$$

Characteristic functions are useful for studying the addition of independent random variables. If random variables A, B, and C satisfy the relationship $C = A + B$ and A and B are independent, then their characteristic functions satisfy the relationship $\Phi_C(v) = \Phi_A(v)\Phi_B(v)$ [Sta94].

Characteristic functions are also useful for studying the superposition of two independent random voltages, such as those in the SLAC model. Since voltage, $\tilde{V}$, is complex-valued, its characteristic function must be a *double* Fourier transform over the joint PDF of the random in-phase, X, and quadrature, Y, voltage components ($\tilde{V} = X + jY$). This transformation is demonstrated below:

$$\Phi_{XY}(v_x, v_y) = \int\limits_{-\infty}^{+\infty}\int\limits_{-\infty}^{+\infty} f_{XY}(x,y)\exp(-jv_x x)\exp(-jv_y y)\,dx\,dy \tag{5.A.3}$$

$$f_{XY}(x,y) = \frac{1}{4\pi^2}\int\limits_{-\infty}^{+\infty}\int\limits_{-\infty}^{+\infty} \Phi_{XY}(v_x, v_y)\exp(jv_x x)\exp(jv_y y)\,dv_x\,dv_y \tag{5.A.4}$$

Starting with the basic envelope PDF, $f_R(\rho)$, as a function of only envelope, ρ, it is possible to extend this PDF into a joint PDF using the relationship

$$f_{R\Phi}(\rho, \phi) = \frac{1}{2\pi\rho} f_R(\rho) \tag{5.A.5}$$

Equation (5.A.5) is a joint PDF, albeit in terms of envelope, ρ, and phase, ϕ, variables instead of in-phase, x, and quadrature, y, variables. Equation (5.A.5) assumes that the net phase, ϕ, is uniformly distributed, independent of ρ - consistent with the I-SLAC model.

Rather than convert Equation (5.A.5) into an XY joint PDF, it is more convenient to make a change of variables in the transform definition of Equation (5.A.3). With the polar-coordinate substitutions $x = -\rho\cos\phi$, $y = -\rho\sin\phi$, and $dx\,dy =$

$\rho \, d\rho \, d\phi$, Equation (5.A.3) becomes

$$\Phi_{XY}(v_x, v_y) = \frac{1}{2\pi} \int\limits_0^\infty \int\limits_0^{2\pi} f_R(\rho) \exp(jv_x\rho\cos\phi) \exp(jv_y\rho\sin\phi) \, d\phi \, d\rho \qquad (5.A.6)$$

Equation (5.A.6) may be grouped:

$$\Phi_{XY}(v) = \int\limits_0^\infty f_R(\rho) \left[\frac{1}{2\pi} \int\limits_0^{2\pi} \exp\left[-jv\rho\cos(\phi + \phi_0)\right] \, d\phi \right] \, d\rho \qquad (5.A.7)$$

where $v = \sqrt{v_x^2 + v_y^2}$ and $\tan(\phi_0) = v_y/v_x$. The angle ϕ_0 is unimportant, since the integration of ϕ_0 is over the entire period of the cosine function in Equation (5.A.7). Thus, the characteristic function is solely dependent on the variable v.

The bracketed term in Equation (5.A.7) is a standard definite integral that evaluates to a zero-order Bessel function of the first kind [Gra94]. The final expression for the transformation from envelope PDF to characteristic function is Equation (5.2.3). Using a similar set of reductions, the reverse transformation from characteristic function to envelope PDF becomes Equation (5.2.4). The only assumption made in these transformations is the statistical independence and uniform distribution of the complex voltage phase.